

# Optimal rotor shape design of 3-step skew spoke type BLAC motor to reducing cogging torque

Sung-An Kim<sup>a</sup>, Gui-Dong Choi<sup>b</sup>, Ju Lee<sup>b</sup> and Yun-Hyun Cho<sup>a,\*</sup>

<sup>a</sup>*Department of Electrical Engineering, Dong-A University, Busan, Korea*

<sup>b</sup>*Department of Electrical Engineering, Hanyang University, Seoul, Korea*

**Abstract.** In electric power steering (EPS), spoke type brushless ac (BLAC) motors offer distinct advantages over other electric motor types in terms of torque smoothness, reliability and efficiency. This paper deals with the shape optimization of spoke type BLAC motor, in order to minimization cogging torque. In this paper examines, 3 step skewing rotor angle, optimizing rotor core edge and rotor overlap length for minimize cogging torque in spoke type BLAC motor. The methods were applied to existing machine designs and their performance was calculated using finite- element analysis (FEA). Prototypes of the machine designs were constructed and experimental results obtained. It is shown that the FEA predicted the cogging torque to be nearly reduce using those method.

Keywords: EPS, 3-step skewing, spoke type BLAC, cogging torque, FEA, optimization

## 1. Introduction

IN recent years, energy savings in vehicles has been issues in the worldwide so that electric vehicles and hybrid electric vehicles, which are driven by electric motors, are being launched in the market. In addition, some hydraulic controlled mechanical systems have been replaced by electric driven systems, such as power steering and brake system. The existing power steering system for vehicles can be categorized into three types, the hydraulic power steering that obtains steering assistant power directly from hydraulic pump driven by the engine, the EPS (Electric Power Steering) that is driven by an electric motor, and the EHPS (Electric Hydraulic Power Steering) that the hydraulic pump for steering assistance is driven by an electric motor. Compared to the hydraulic power steering system, the EPS has shown better fuel efficiency, better steering feel, and environment friendly, reduced manufacturing time on the production line, and it also offers more space in engine compartment due to the down-sizing with the reduced component [13–15].

Due to these benefits, the EPS shared about 35% of the power steering world market in 2007 and its portion in the market share has been continually increased [14]. Moreover, cogging torque is one of the important drawbacks of EPS, spoke type BLAC motors, which results in shaft vibration and noise.

---

\*Corresponding author. Yun-Hyun Cho, Department of Electrical Engineering, Dong-A University, Busan, Korea. Tel.: +82 51 200 7742; Fax: +82 51 200 7743; E-mail: yhcho@dau.ac.kr.

Table 1  
Main design parameters for prototype

Symbol	Item	Unit	Value
$P$	Phase number	–	3
$D_{so}$	Stator outer diameter	mm	88.8
$D_{ro}$	Rotor outer diameter	mm	50.8
$l_a$	Stack length	–	39
$p_s$	Stator slot number	–	12
$p_r$	Rotor slot number	–	8
$N_{coil}$	Coil turn number	–	24
$PM$	Magnet Material	–	Ferrite
$g$	Air gap length	mm	0.62
$\tau$	Skewing step number	–	3
$N_p$	No. of poles	–	8
$T_r$	Rated Torque	Nm	3.26
$P_w$	Rated power	Watt	420
$N_r$	Rated rotational speed	rpm	1230
$V$	Voltage	Volt	12
$A$	Current	Amp.	70

Particularly, cogging torque causes pulsating in motor torque and prevents having a smooth rotation, especially at low speeds and light loads. The cogging torque and its reduction techniques in PM brushless AC machines have been broadly investigated over the past decades. Up to date, there have been various studies devoted to 3-D analytical modeling and prediction of cogging torque in surface-mounted PM brushless machines with regular geometric shapes [6,7] and the versatile finite-element analysis (FEA) is widely employed to evaluate the cogging torque in all kinds of PM brushless AC machines [8,9]. Recently brushless spoke type machines are becoming increasingly popular in industrial applications. They offer a highly efficient, high power-density, low size alternative to conventional machines, and as their cost continues to decrease they have the opportunity to become a dominant force in the industrial applications market [1,2]. One major drawback to spoke type machines is the torque ripple that is inherent in their design. This ripple is parasitic, and can lead to mechanical vibration, acoustic noise, and problems in drive systems. Minimizing this ripple is of great importance in the design of a BLAC spoke type machine [3].

However, in many case of vehicle applications, a cogging torque of the electric motor is of basic concern. There is no exception for the BLAC motor employed as the EPS system.

Therefore, the cogging torque minimization of the BLAC motor is becoming necessary since its low torque ripple is required in the EPS application. This paper presents the rotor Shape optimization of a 3-step skewing [5] spoke type BLAC motor, which is designed for an electric power steering application. The design specification of the BLAC motor for the EPS application is listed in Table 1, and proto type of the spoke type BLAC motor is illustrated in Fig. 1(a).

## 2. Study on reducing cogging torque

### 2.1. Cogging torque reduction technique

In its most fundamental form, cogging torque can be represented by

$$T_{cog} = -\frac{1}{2}\varphi_g^2 \frac{dR}{d\theta} \quad (1)$$

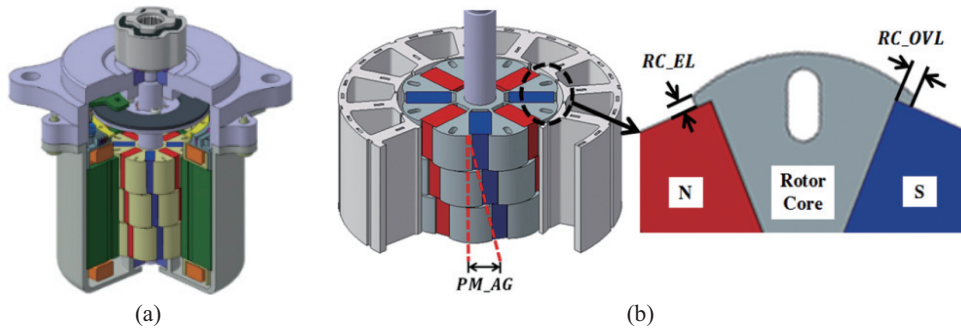


Fig. 1. (a) Proto type 3-step skewing spoke type BLAC Motor, (b) Rotor Skew model for minimizing cogging torque.

Where  $\phi_g$  is the air-gap flux,  $R$  is the air-gap reluctance, and  $\theta$  is the position of the rotor [1]. This supports the idea that cogging torque is the interaction between the magnets (the source of the air-gap flux since cogging torque is considered with an unexcited stator) and the stator teeth (the source of the varying air-gap reluctance). The air-gap reluctance varies periodically, thus causing the cogging torque to be periodic [7]. Because of this periodicity, cogging torque can be expressed as a Fourier series:

$$T_{cog} = \sum_{k=1}^{\infty} T_{mk} \sin(mk\theta) \quad (2)$$

Where  $m$  is the least common multiple of the number of stator slots ( $p_s$ ) and the number of poles ( $N_p$ ),  $k$  is an integer, and  $T_{mk}$  is a Fourier coefficient [2]. It is seen that the cogging torque has  $m$  periods per mechanical revolution of the rotor and has a direct relationship to the number of slots and poles.

To theoretically eliminate cogging torque via machine design, one must examine the equations that define it. From the inspection of Eq. (1), it is seen that cogging torque can be eliminated by forcing either the air-gap flux,  $\phi_g$  or the rate of change of the air-gap reluctance,  $dR/d\theta$  to be zero. Making  $\phi_g$  zero is not possible since the air-gap flux is needed for the alignment and reluctance torque components that drive the machine. Therefore, cogging torque can be cancelled by forcing the air-gap reluctance to be constant with respect to rotor position. In practice, cogging torque cannot be easily eliminated, but it can be greatly reduced [1]. Examination of Eq. (2) reveals that cogging torque can be represented as a Fourier series so it is a summation of harmonic sinusoids. In traditional machines with no cogging torque reduction design techniques, the rotor magnets have an additive effect when contributing to cogging torque because each magnet has the same relative position with respect to the stator slots [2]. The torque from each magnet is in phase with the others, and thus the harmonic components of each are added. By designing a machine in such a way that the cogging effects from the magnets are out of phase with each other, some of the harmonics seen in Eq. (2) can be eliminated, thus reducing cogging torque. An alternative is to skew the rotor. With a full-ring magnet this can be done by imposing a skewed magnetization pattern, using a magnetizing fixture with skewed poles. With arrays of magnets such as shown in Fig. 2. This supports the idea that cogging torque is the interaction between the magnet and the stator teeth. Therefore it is possible to reducing cogging torque by changing rotor skew model and rotor pole shape. Whether it is applied to the rotor, skewing reduces the winding factor and the fundamental EMF by the so-called skew factor. The following design technique is a combination of methods that utilize the aforementioned cogging torque reduction theories. It should be noted that although these techniques are successful in reducing the undesired cogging torque, when used alone, they also reduce the desired mutual torque. Along with the higher manufacturing costs associated with the generally more complex machine designs, these are the two main tradeoffs in reducing cogging torque [1].

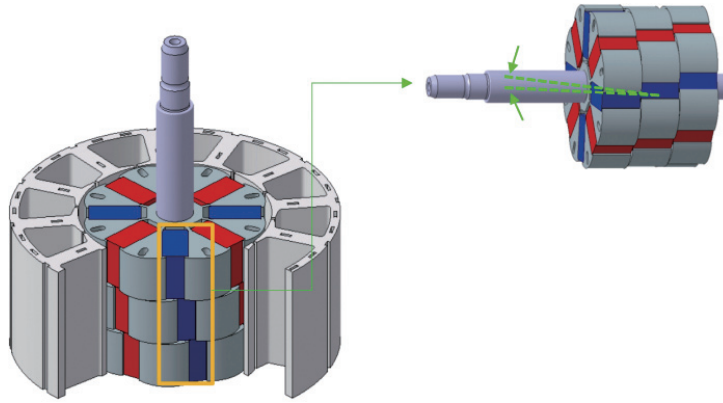


Fig. 2. Rotor Skew model for minimizing cogging torque.

### 3. Decision of design variables

The combination of rotor pole [18] number and stator slot number can be optimized to reduce the cogging torque in PM brushless AC machines. Moreover, in this paper other cogging torque minimization techniques can be mainly categorized of rotor design. The rotor design based include rotor core edge length (RC\_EL), rotor overlap length (RC\_OVL) and PM rotor step skew angle (PM\_AG) are illustrated in Fig. 1(b). However, it is usually more preferable to implement rotor design based techniques than the stator design based ones to reduce the cogging torque due to the simpler rotor structure in PM brushless AC machines. The cogging torque could be virtually eliminated by uniformly 3 steps skewing the stator slots by the angle of one cogging torque period, which is rather difficult to implement in the wound stator.

Alternatively, continuously step skewing the simpler rotor by the same angle could be employed instead with equivalent results. However, continuous rotor skewing will inevitably results in magnets with irregular shapes, which are normally very expensive and even impractical to fabricate and magnetize. Consequently, a variant and alternative from called rotor 3 step skewing, which skews the rotor axially by certain discrete steps and hence eases the construction and assembly of the rotor. Rotor skewing techniques are common practices in industry for cogging torque and torque ripple minimizations of PM brushless machines. Skewing the rotor magnet continuously is not convenient and even impractical for the prototype machine due to its shaped magnet poles. Therefore, skewing the rotor magnet stepwise is more preferable to ease fabrication and assembly. The cogging torque waveforms of the machine with different steps are comprehensively evaluated by FEA for rotor step skewing techniques. By neglecting axial-coupling effects between the steps and the end effects, the overall cogging torque of the machine with rotor step skewing techniques can be obtained by synthesizing the cogging torque produced by FEA results as shown in expression Eq. (3) [5]

$$T_c(\theta) = \sum_{n=1}^{\infty} \sum_{k=0}^{p_s-1} \frac{\sin\left(\frac{\tau}{2} n p_r \theta_s\right)}{\tau \sin\left(\frac{n}{2} p_r \theta_s\right)} \cos\left(\frac{2k n p_r \pi}{p_s}\right) T_{c s n} \sin(n p_r \theta_s) \quad (3)$$

Where  $\tau$  and  $\theta_s$  are the skewing step number and mechanical skewing angle between the adjacent two steps. By inspection, all the harmonics of the cogging torque can virtually be eliminated except those which are multiples of  $\tau$  with the step skewing angle as:

$$\theta_s = \frac{2k\pi}{\tau l c m(N_r, p_s)}, k = 1, 2, 3 \dots \quad (4)$$

Table 2  
Design variable for spoke type BLAC motor

Design variable	Items	Variable Range	Unit
$x_1$	Permanent magnet skew angle ( $PM\_AG$ )	$6^\circ \sim 14^\circ$	deg.
$x_2$	Rotor core edge-length ( $RC\_EL$ )	$1.0 \sim 1.5$	mm
$x_3$	Rotor overlap length ( $RC\_OVL$ )	$1.9 \sim 2.4$	mm

Table 3  
Observed responses obtained by FEM

No.	$x_1$ (degree)	$x_2$ (mm)	$x_3$ (mm)	$Y_{BEMF}$ (V)	$Y_{CogT}$ (Nm)
1	$14^\circ$	1.25	2.15	2.15	0.01230
2	$6^\circ$	1.50	2.40	3.01	0.02500
3	$10^\circ$	1.25	1.90	1.75	0.00950
4	$6^\circ$	1.25	2.15	1.95	0.01230
5	$14^\circ$	1.50	1.90	2.10	0.02500
6	$10^\circ$	1.25	2.15	1.62	0.00723
7	$6^\circ$	1.50	1.90	1.56	0.00780
8	$6^\circ$	1.00	1.90	1.56	0.00780
9	$6^\circ$	1.00	2.40	1.56	0.00780
10	$14^\circ$	1.00	2.40	1.86	0.00850
11	$10^\circ$	1.50	2.15	1.95	0.00900
12	$14^\circ$	1.00	1.90	1.96	0.19000
13	$10^\circ$	1.25	2.40	1.82	0.09500
14	$14^\circ$	1.50	2.40	1.75	0.01200
15	$10^\circ$	1.00	2.15	2.20	0.00980

$Y_{BEMF}$  = Coefficient of Back-EMF (BEMF),  $Y_{CogT}$  = peak to peak of cogging torque.

Where  $k$  normally should be kept as small as unity in order to prevent the machine performance from excessive deterioration. Based on the 2-D FEA results, the initial cogging torque and after optimization waveform of the machine with rotor 3 step skewing and corresponding step skewing angle from Eq. (4) is derived in Fig. 1(b).

## 4. Optimization technique by using RSM method

### 4.1. Response surface methodology

Improving quality is important goal in any research. The methods for determining how to improve quality are evolving. They have changed from costly and time-consuming trial-and error searches to the powerful, elegant, and cost-effective statistical methods. One of these methods is Design of Experiments (DOE) [17]. DOE is centered on factors, responses, and runs. DOE helps to determine if and how a factor affects a response. In this paper Response Surface Method (RSM) [16] which is one of DOE branches is used as optimization Method.

The Cogging torque of the spoke type BLAC motor is complicated due to the influence of excessive magnetic saturation. Therefore, the finite element method (FEM) is adopted as a magnetic field analysis method, and the computational optimization has become indispensable for the electric machine design [4,9,10]. Therefore, in the proposed approach, the FEA is employed to analysis a magnetic field of the BLAC motor, the response surface method (RSM) is used to formulate the objective to reduce the cogging torque. The RSM is well adapted to make a systematic model for a complex problem, and the RSM provides a response surface of the overall behavior of design variables within a design space. In

Table 4  
Comparison between initial shape and optimum shape

Parameter	Unit	Initial designed motor	Optimum designed motor
$x_1$	mm	6.0°	6.30°
$x_2$	mm	1.2	1.21
$x_3$	mm	2.0	1.93
BEMF	V	1.37	1.58
Cogging torque	N-m	0.017	0.0080

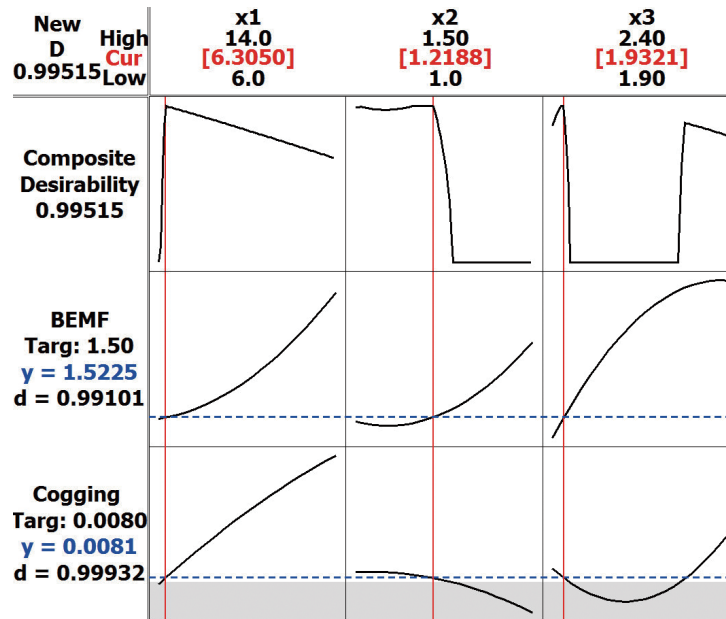


Fig. 3. Optimization analysis of BEMF and Cogging Torque in RSM.

order to apply RSM technique for optimization the method describes in details in [11,12] are utilized. The expression of response surface is commonly used as a second-order polynomial representation and it can be written as follows:

$$y = \beta_0 + \sum_{i=1}^n \beta_i x_i + \sum_{i=1}^n \beta_{ii} x_i^2 + \sum_{i \neq j}^n \beta_{ij} x_i x_j + \varepsilon \tag{5}$$

Where  $n$  is the number of design variables,  $\beta$  is regression coefficients,  $\varepsilon$  denotes the error estimate, and  $y$  can be the cogging torque, the coefficient of the back-EMF from the configuration of the initial shape of the motor shown in Fig. 1(b), three design variables are chosen for the reduction of the cogging torque. The design parameters, from  $x_1$  to  $x_3$ , are described in Table 2.

The design-space to make an appropriate response surface model is screened in Table 3. From the design-space, designs of experimental (DOE) are listed in Table 2.

A central composite design (CCD), which is one of DOE, is applied to obtain the approximate selection of the calculating points, because of providing a systematic and efficient approach in order to build the second-order fitted model. The next step in design process for the reduction of the cogging torque is to apply an optimization procedure.

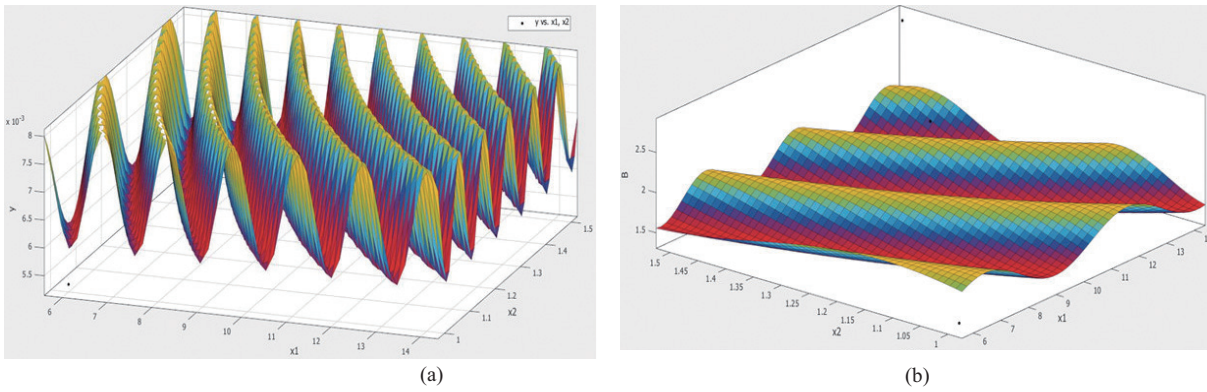


Fig. 4. (a) Response surface cogging torque (b) Response surface BEMF.

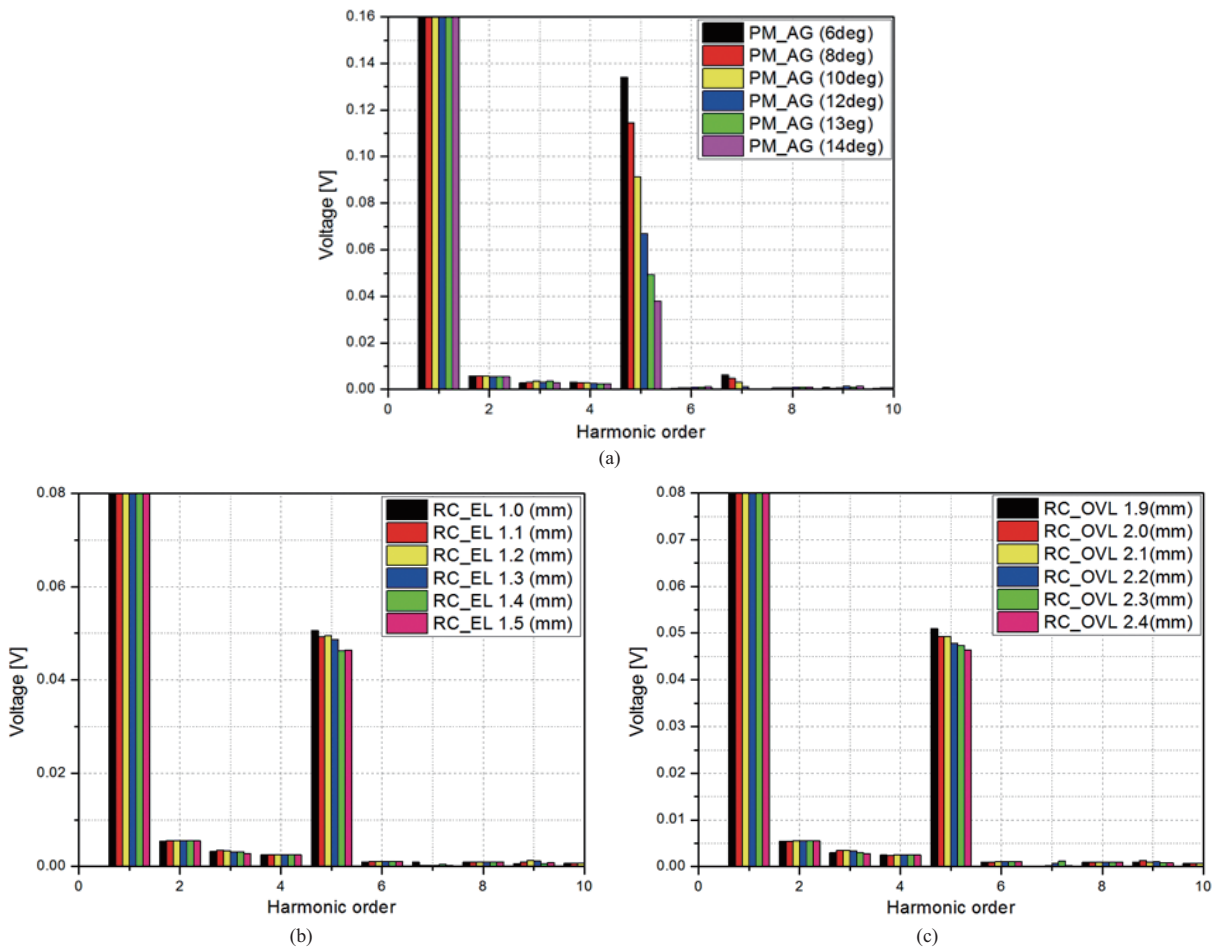


Fig. 5. Back EMF FFT for (a) various Permanent magnet skew (b) various Rotor core Edge Length(c) various Rotor overlap Length.

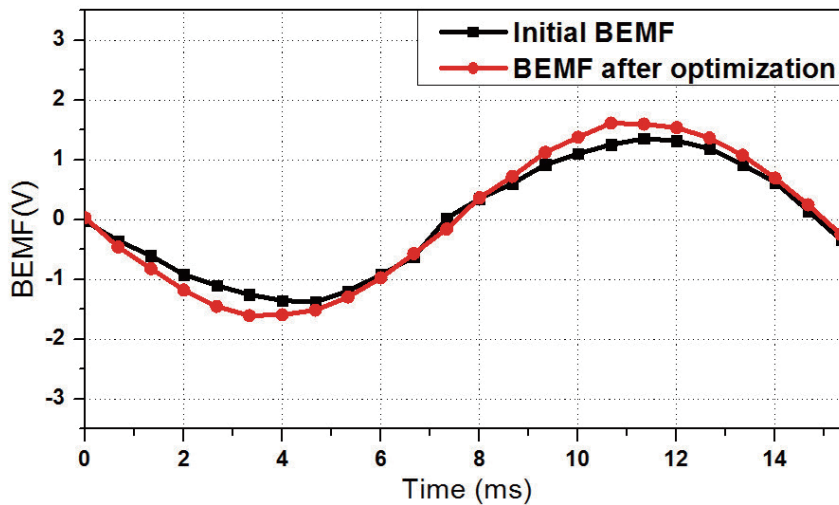


Fig. 6. BEMF comparison between initial model and after optimization.

The constrained optimization problem can be written mathematically as follows:

Minimize:

$$f(x) = Y_{cogT} = 0.02315x_1^2 + 0.188x_1x_2 - 0.3412x_1x_2 - 0.03789x_1 - 4.613x_2^2 + 4.709x_2x_3 + 2.006x_2 + 0.001825x_3^2 - 0.03122x_3 + 0.8408$$

Where  $f(x)$  is the objective function and  $f(x)$  is estimated by the response surface model of the peak to peak value of the cogging torque.

## 5. Results and discussion

The prediction of the second order polynomial models, which is obtained by the RSM, is illustrated in Fig. 3. In order to minimize the cogging torque in the design space, the value of rotor step skew angle, rotor core edge length, rotor overlap length depth turned out to be an existence. Figure 4(a) shows the response surface of the cogging torque and (b) shows the coefficient of back EMF at 1230 rpm according to design variables respectively. From the response surfaces of the cogging torque, the two local minimum areas turned out to be an existence. After optimization with response surface method we get our optimum point for spoke type BLAC motor. The results of computational optimization compared with the results of the initial design are shown in Table 4.

These results compare very well with those obtained using FEA analysis directly. The results of the FEA analysis correspond to optimum design variables, which is the cogging torque, torque ripple and torque curves shown in Fig. 7 and the BEMF comparison between initial designs and after optimization design waveform shown in Fig. 6. The harmonic are analyzed by fast Fourier transform (FFT), as shown in Fig. 5 back EMF for (a) various PM skew (b) various rotor core edge length (c) various rotor overlap length respectively.

The P-P cogging torque value can be reduced from 0.017 to 0.0080 Nm (nearly 53%) by rotor optimization. Therefore the results of the optimum design for the cogging torque reduction are contented with the demanded motor specification for the EPS application.



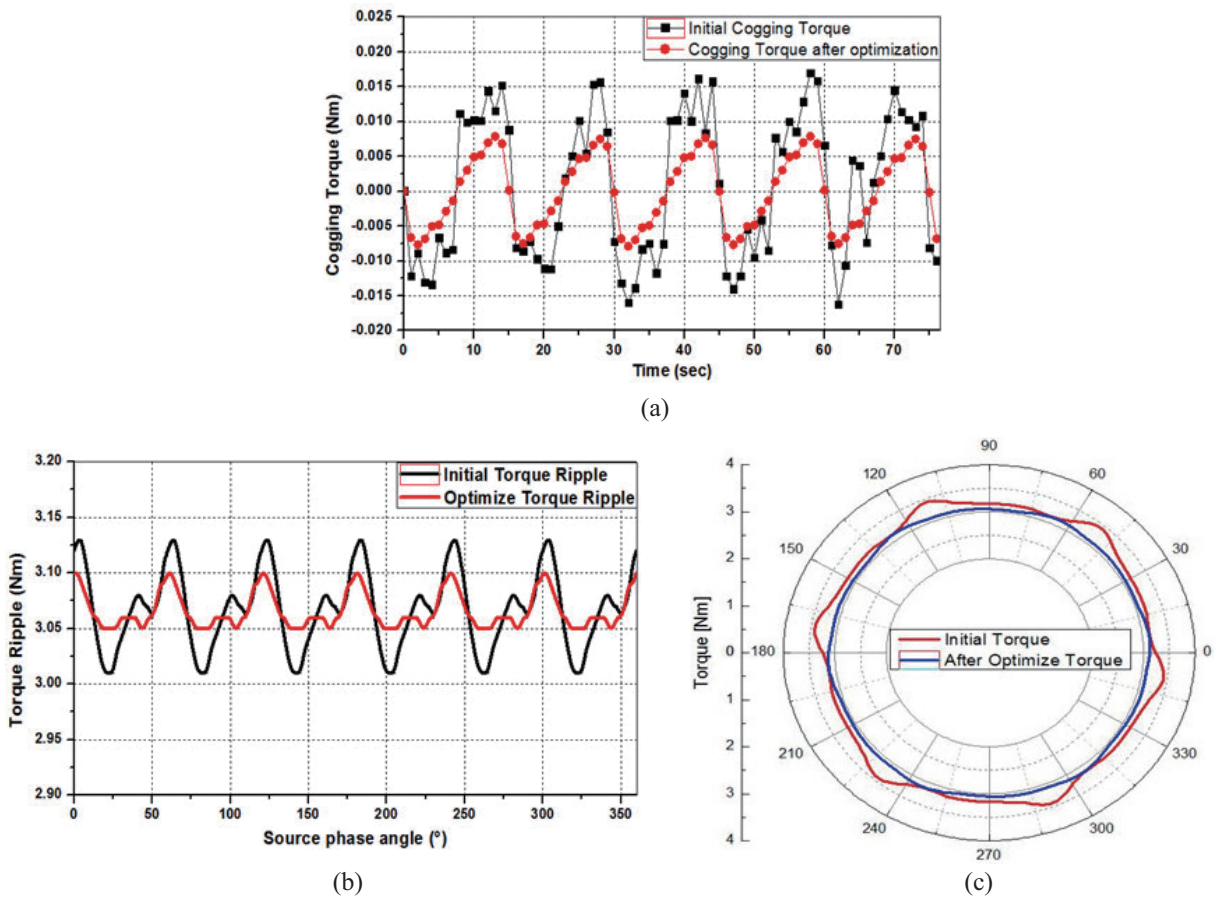


Fig. 7. Comparison between Initial model and after optimization(a) cogging torque(b) torque ripple (c) and torque respectively.

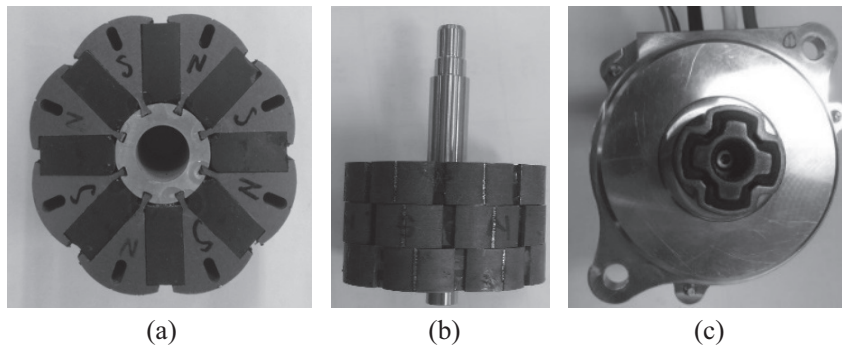


Fig. 8. (a) Optimized rotor shape (b) Three step rotor skew (c) Assembled prototype of Spoke type BLAC.

## 6. Experimental results

The spoke type BLAC motor with optimized rotor has been prototyped for the experimental validation of the FEA results and the verification of the rotor optimization techniques for cogging torque minimiza-

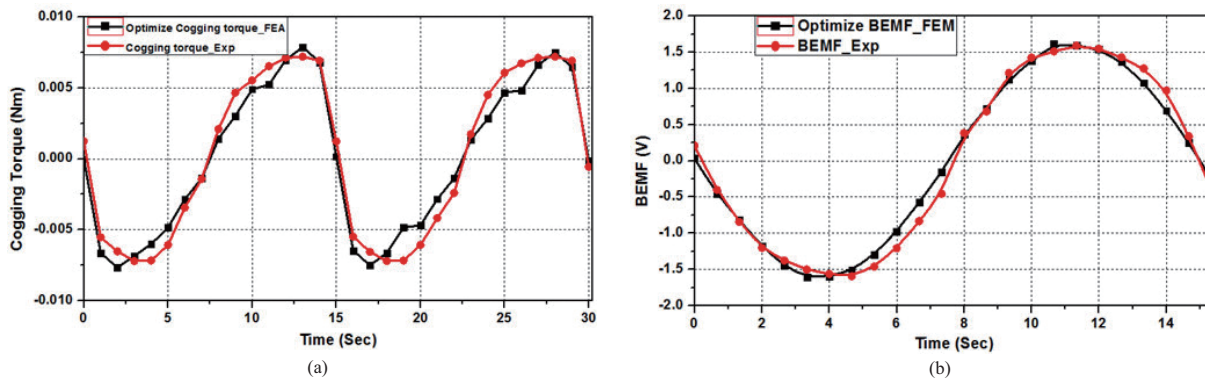


Fig. 9. Comparison of (a) cogging torque and (b) BEMF waveforms of the 3-D FEA and experimental results.

tion. Figure 8 shows the photos of (a) optimized rotor shape (b) three step rotor skew and (c) assembled prototype. The measured and 3-D FEA predicted (a) cogging torque and (b) BEMF waveforms of the prototype are compared in Fig. 9. However, comparison results confirmed that cogging torque is reasonably good agreement as well BEMF. The measured cogging torque from the machine with optimize rotor is about similar than the 3-D FEA estimated one. Therefore the agreement of the predicted and measured cogging torque result is considered satisfactory. Furthermore, an alternative current motor has been used to drive the rotor of the prototype machine at rated speed in order to measure the back EMF waveforms. It can be found from Fig. 9(b) that is relatively close agreement between the predicted and measured result.

## 7. Conclusion

This paper described the shape optimization in order to reduce the cogging torque in the SPOKE type BLAC motor. The experimental results obtained from the prototype demonstrate satisfactory agreement with the estimated by FEA approaches, and underpin the findings of the study. And optimum design for the cogging torque reduction are satisfied with the required motor specification for the EPS application.

## Acknowledgments

This research was supported by Basic Science Research Program through the National Research Foundation of Korea (NRF) grant funded by the Korea Government (MSIP) No: NRF-2014R1A2A2A 01003368) and by the Human Resources Development of the Korea Institute of Energy Technology Evaluation and Planning (KETEP) grant funded by the Ministry of Knowledge Economy, Republic of Korea under Grant 20134030200320.

## References

- [1] D. Hanselman, *Brushless Permanent-Magnet Motor Design*. NewYork: McGraw-Hill, 1994.
- [2] C. Bretón, J. Bartolomé, J.A. Benito, G. Tassinario, I. Flotats, C.W. Lu and B.J. Chalmers, Influence of machine symmetry on reduction of cogging torque in permanent magnet brushless motors, *IEEE Trans. Magn.* **36**(5) (Sep. 2000), 3819–3823.

- [3] Z.Q. Zhu and D. Howe, Influence of design parameters on cogging torque in permanent magnet machines, *IEEE Trans. Energy Convers* **15**(4) (Dec. 2000), 407–412.
- [4] S. Wakao, T. Onuki, J.W. Im and T. Yamamura, A novel design approach for grasping broad characteristics of magnetic shield problem, *IEEE Trans. Magn.* **34**(4) (July 1998), 2144–2146.
- [5] W. Fei and Z.Q. Zhu, Comparison of cogging torque reduction in PM brushless machines by conventional and herring-bone skewing techniques, *IEEE Trans. Energy Convers.* **28**(3) (Sep. 2013).
- [6] Z.Q. Zhu and D. Howe, Analytical prediction of the cogging torque in radial-field permanent magnet brushless motor, *IEEE Trans. Magn.* **28**(2) (Mar. 1992), 1371–1374.
- [7] J.F. Gieras, Analytical approach to cogging torque calculation of PM brushless motor, *IEEE Trans. Ind. Appl.* **40**(5) (Sep./Oct. 2004), 1310–1316.
- [8] J.A. Guemes, A.A. Iraolagoitia, J.J. DelHoyo and P. Fernandez, Torque analysis in permanent-magnet synchronous motors: a comparative study, *IEEE Trans. Ind. Appl.* **47**(3) (May/Jun. 2011), 1247–1256.
- [9] S.-M. Jin, Y.-W. Zhu and Y.-H. Cho, Optimal design of auxiliary poles to minimize detent force of permanent magnet linear synchronous motor, *International Journal of Applied Electromagnetics and Mechanics* **33**(1–2) (2010).
- [10] Y. Fujishima, S. Wakao, M. Kondo and N. Terauchi, An optimal Design of Interior Permanent Magnet Synchronous Motor for the Next Generation Commuter Train, *IEEE Trans. Magn.* **14**(2) (2004), 1902–1905.
- [11] Y.-W. Zhu, S.-G. Lee and Y.-H. Cho, Optimal design of PMLSM with low force pulsations using response surface methodology, *Applied Electromagnetics and Mechanics* **34** ISBN, 2010.
- [12] Z.-L. Gaing, C.-H. Lin, M.-H. Tsai and M.-C. Tsai, Rigorous design and optimization of brushless PM motor using response surface methodology with quantum behaved PSO operator, *IEEE Trans. Magn.* **50**(1) (January 2014).
- [13] A.W. Burton, Innovation drives for electric power assisted steering, *IEEE control systems Magazine*, Nov. 2003, pp. 30–39.
- [14] H. Eki, T. Teratani and T. Iwasaki, Power consumption and conversion of EPS systems, *Power Conversion Conference (PCC)*, 2007, pp. 1333–1339.
- [15] G. Ombach and J. Junak, Two rotors designs comparison of permanent magnet brushless synchronous motor for an electric power steering application, *European Conference on Power Electronics and Applications (EPE)*, 2007, pp. 1–9.
- [16] R.H. Myers and D.C. Montgomery, *Response Surface Methodology Process and Product Optimization Using Designed Experiments*, New York: Wiley, 1995.
- [17] D.C. Montgomery, *Design and Analysis of Experiments*, New York: Wiley, 2001.
- [18] C. SeopKoh, Magnetic Pole Shape Optimization of PM motor for Reduction of Cogging Torque, *IEEE Trans. Magn.* **33**(2) (March 1997).